

Structural and Electrical Properties of Ferroelectric Bismuth Titanate Thin Films Prepared by the Sol Gel Method

M. Sedlar & M. Sayer

Department of Physics, Queen's University, Kingston, Ontario, Canada, K7L 3N6

(Received 5 May 1995; accepted 12 June 1995)

Abstract: Crystalline bismuth titanate films were fabricated using a modified sol gel method. The process was simplified using stock titanium and bismuth solutions. Films were fabricated using rapid thermal processing with a ramp rate of 100°C/s to 700°C for 30 s. The average grain size of films was 175 nm. A dielectric constant in the typical range of 220 and $\tan\delta$ of 0.01 were measured. P - E hysteresis loops were observed with the ferroelectric properties of $P_s = 22 \mu\text{C}/\text{cm}^2$, $P_r = 10 \mu\text{C}/\text{cm}^2$ and the coercive force $E_c = 165 \text{ kV}/\text{cm}$. The leakage current density was of the order of $10 \text{ nA}/\text{cm}^2$ at $60 \text{ kV}/\text{cm}$. An almost flat C - V characteristic and a charge storage density of $42 \text{ fC}/\mu\text{m}^2$ at $220 \text{ kV}/\text{cm}$ were measured.

1 INTRODUCTION

Bismuth titanate $\text{Bi}_4\text{Ti}_3\text{O}_{12}$ is a ferroelectric material, which in thin film form can be used for ferroelectric or electro-optic devices.¹ High Curie temperature $T_c = 675^\circ\text{C}$, excellent fatigue behaviour and reasonable ferroelectric properties make bismuth titanate an attractive candidate for ferroelectric (FERRAM) or dynamic (DRAM) random access memories.¹ Bismuth titanate films formed on a superconductor showed promising ferroelectric properties and the potential for integration into semiconductor device processing technology.²

$\text{Bi}_4\text{Ti}_3\text{O}_{12}$ thin films have been prepared by various techniques such as pulsed laser ablation,³ MOCVD⁴ and sol gel.^{5–7} Large-scale processing in the IC industry requires low-temperature synthesis, high reproducibility and relative simplicity of all processing steps. Sol gel methods seem to fulfil these requirements as they offer excellent composition control, low-temperature processing and short fabrication times at comparatively low cost. However, sol gel $\text{Bi}_4\text{Ti}_3\text{O}_{12}$ films^{5–7} synthesized so far have used a conventional furnace heat-treatment, which may have an adverse effect on the

metal–film interface, thereby degrading electrical properties. Problems with the separation of the Bi_2O_3 phase influencing the final properties have also been encountered.⁶ In this paper we describe a modified sol gel method, which simplifies the preparation procedure and contributes to higher reproducibility. The chemistry of the process and the effect of rapid thermal processing (RTP) on the crystallinity and electrical properties are also discussed.

2 EXPERIMENTAL

Bismuth nitrate $\text{Bi}(\text{NO}_3)_3 \cdot 5\text{H}_2\text{O}$ was dissolved in concentrated nitric acid or glacial acetic acid, diluted and mixed with titanium stock solution. The latter solution consists of titanium isopropoxide, acetylacetone and methoxyethanol mixed in the molar ratio 1/1/4. The clear solution was diluted with a mixture of water and methoxyethanol. Filtered solutions were dispensed from a syringe using a $0.2 \mu\text{m}$ syringe filter and were spun on to various substrates (platinized silicon wafer $\text{Si}/\text{SiO}_2/\text{Ti}/\text{Pt}$, RuO_x , ITO) at a rotation speed of 4000 rpm for 30 s. The green films were then fired

at 300°C on a hot plate and heat-treated in a rapid thermal processor (AG Associates Heatpulse 410) at 550–750°C for 30–180 s.

The crystallographic structure of films was analysed using a Rigaku Miniflex X-ray diffractometer (CuK_α anode) and by glancing angle XRD (Rigaku D-Max goniometer attached to a 12 kW rotating anode generator). Scanning electron microscopy (SEM) was used to study the surface morphology of the films. Thickness measurement and size distribution of crystallites throughout the film was done using transmission electron microscopy (TEM). For the electrical characterization, the capacitor area was defined by top gold or aluminium electrodes, which were deposited by evaporation (Edwards coating system Auto E306A). Low field and bias measurements were carried out using a HP4284A LCR meter with an oscillation level of 50–100 mV. A Sawyer–Tower circuit attached to a HP54501A digital oscilloscope was used to measure the ferroelectric properties (1 kHz). A probe system attached to a Keithley 236 source measure unit was used to measure the leakage current of the films.

3 RESULTS AND DISCUSSION

3.1 Solution chemistry

We examined the solution chemistry of the bismuth titanate system with the aim to prepare a stable, i.e. moisture-insensitive, solution. In other words, we require a system with a fixed viscosity that never gels in the container. However, it must gel after the deposition of a layer of uniform thickness. We have previously discussed the problem of homogeneity in multicomponent ceramic films.⁸ The best homogeneity can be achieved when the solution species are uniform in size and of dimensions comparable to that of a characteristic volume containing all elements required to produce a stoichiometric compound. Consistency of species size can be maintained by using a chelating agent such as acetylacetone. The estimated size of the species present within a titanium stock solution is less than 0.3 nm according to dynamic light scattering experiments. Upon addition of 4 moles of water (4 moles of H_2O per mole of alkoxide, i.e. $r_w=4$) the particle size increased up to 2.2 nm with narrow size distribution. After the addition of 16 moles of water, only a slight increase up to 2.7 nm was detected, indicating excellent stability of the titanium modified precursor. As the titanium stock solution does not destabilize⁹ for $r_w < 50$, relatively high quantities of water can be added to substitute

for other solvents and to substantially reduce the sensitivity to ambient moisture.

Bismuth nitrate as a viable bismuth precursor hydrolyses, giving rise to the acidic reaction. This fact would imply a water-free environment to obtain a clear stable solution. However, if a small quantity of concentrated nitric acid (2:1 in weight) is used to dissolve the bismuth nitrate, subsequent water addition is possible. A comparatively large amount of water can be added ($r_w=20$) without either gelation of the titanium precursor or precipitation of $\text{Bi}(\text{OH})_3$. For example, a solution having a ratio $r_w=10$ was stable over a period of several months, while a solution of $r_w=40$ precipitated after several days. We have previously shown that the stability of acetylacetonates against condensation can be further increased by supplying free protons, i.e. by adding a strong acid.⁹ This is understood in terms of the electrostatic stabilization, where charged species mutually repel each other, thereby preventing the system from excessive association. Higher water quantities can then be used to substitute for the organic solvent and to control the viscosity. Glacial acetic acid was also found to be an efficient agent to dissolve $\text{Bi}(\text{NO}_3)_3$. In this case, however, the quantity of acetic acid must be greater, as it is a weaker acid and its molecules also react with the titanium alkoxide. According to Yi,¹⁰ for the PZT (lead zirconate titanate) water-based system, the viscosity is controlled by the addition of proper amounts of water and acetic acid. Lactic acid can be further added to improve the stability. $\text{Bi}(\text{NO}_3)_3$ and acetic acid were mixed in a molar ratio 1:14 and added to the titanium isopropoxide modified by lactic acid ($r_{la}=1$). Water and methoxyethanol ($r_w=18$, $r_m=10$) were then used to compose the optimized bismuth titanate solution. The particle size in the ‘acetic acid’ based system is expected to be larger¹⁰ than that of ‘acetylacetone’ system, thereby affecting the gel microstructure. It was observed that

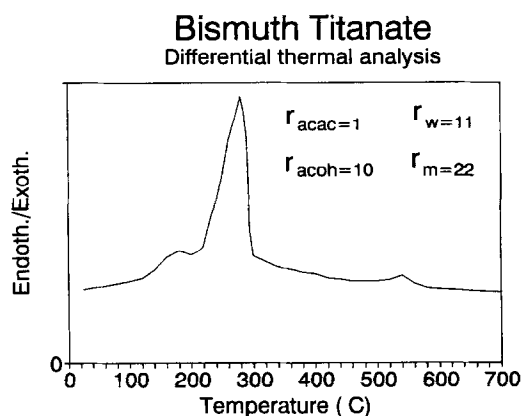


Fig. 1. Differential thermal analysis of the bismuth titanate gel.

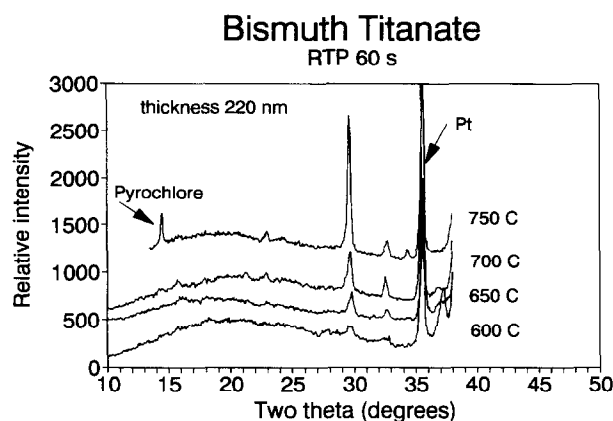


Fig. 2. X-ray diffraction patterns of the bismuth titanate films processed at various temperatures using rapid thermal processing for 1 min.

films deposited from an 'acetic acid' solution were more prone to crack when directly exposed to temperatures over 600°C in a rapid thermal processor.

Figure 1 shows the result of the differential thermal analysis (DTA) experiment carried out for the bismuth titanate gel with a molar ratio of water/acetic acid/methoxyethanol of 11/10/22. The first exotherm was likely due to the decomposition of bismuth nitrate, while the second broad exothermic peak around 280°C was due to the combustion of alkyl groups and pyrolysis of acetylacetonate rings. A less pronounced exothermic peak at 550°C can be attributed to the formation of the crystalline phase.

3.2 Crystallinity and microstructure

Using conventional furnace annealing we were able to obtain the first indication of the crystalline phase above 550°C. Fully crystallized films developed at 650°C after 1 h of annealing, but films often showed an increased fraction of pyrochlore

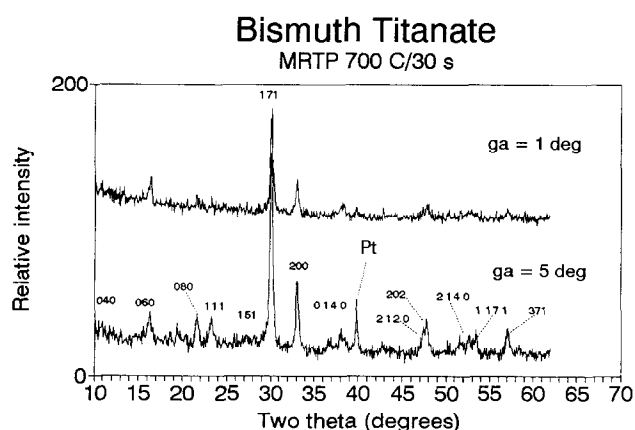


Fig. 3. Glancing angle X-ray diffraction of bismuth titanate film surface. No pyrochlore phase found.

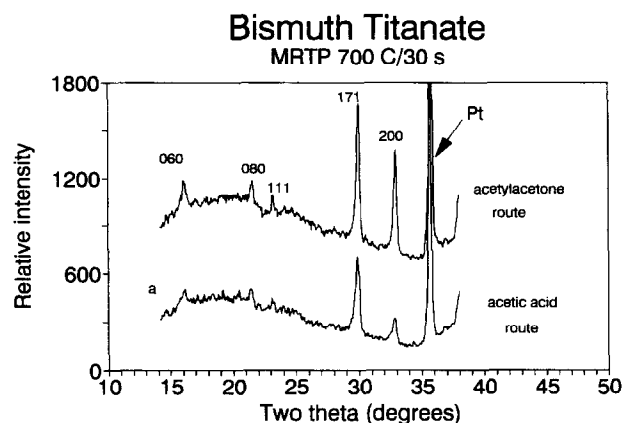


Fig. 4. X-ray diffraction of bismuth titanate films prepared using different starting precursors and processed at 700°C/30 s. Acetylacetonate route gave rise to better crystallized films compared to acetic acid route.

phase $\text{Bi}_2\text{Ti}_2\text{O}_7$. The onset of crystallization using rapid thermal processing (RTP) has been found to be somewhat shifted to the higher temperature. Figure 2 shows a crystalline phase evolution of the bismuth titanate films with the temperature using a linear ramp rate of 100°C/s. Processing the whole film at 700°C for 60 s seemed to be sufficient to crystallize the film, while processing at a temperature of 750°C induced the formation of the pyrochlore. Therefore, 3% of $\text{Bi}(\text{NO}_3)_3$ in excess were subsequently used to compensate for the bismuth loss during thermal annealing. The examination of the film surface by glancing angle XRD ($\Theta = 1^\circ$ and 5°) did not show any phases other than the orthorhombic $2\text{Bi}_2\text{O}_3 \cdot 3\text{TiO}_2$ phase (Fig. 3). The lattice constants a , b and c were calculated using the (200), (171) and (111) peaks and were found to be 5.42, 32.79 and 5.49 Å, respectively, which are consistent with the values given in the JCPDS (no. 35795) data card. The effect of the chemistry on crystalline phase evolution is documented in Fig. 4.

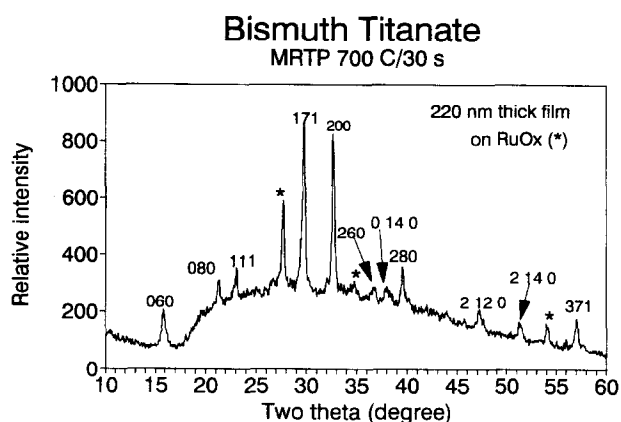


Fig. 5. X-ray diffraction of the bismuth titanate films deposited on ruthenium oxide electrode. A slight preferential orientation in the {200} direction was observed.

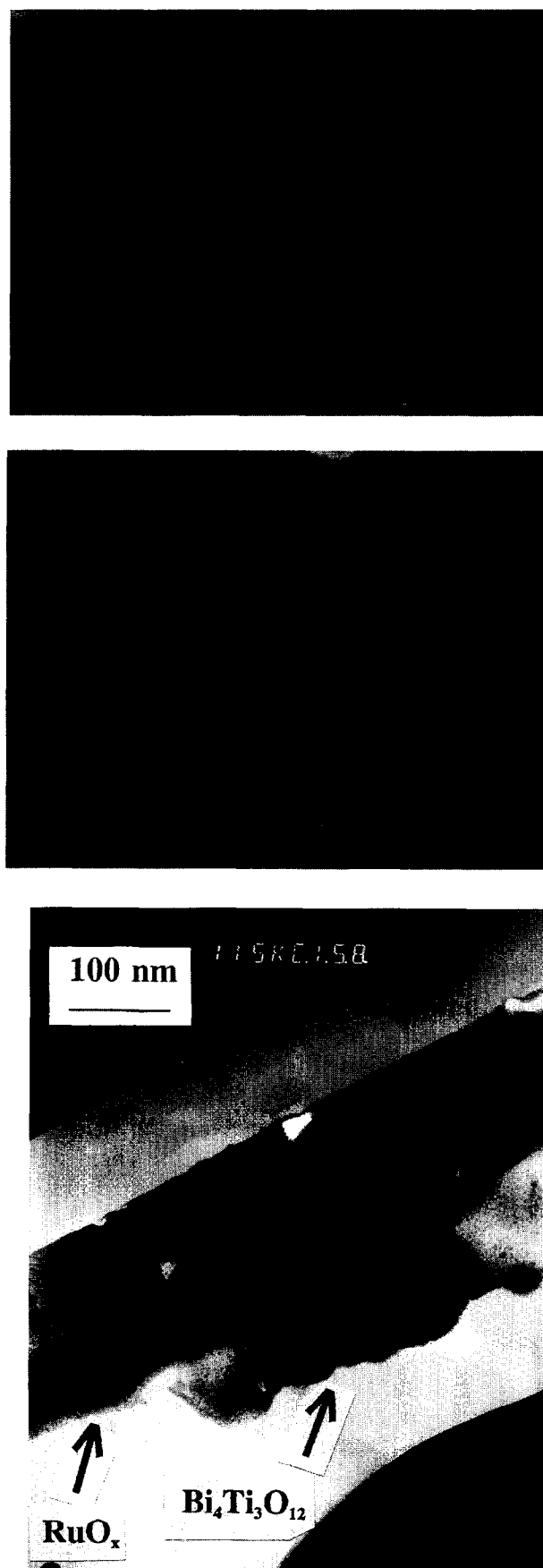


Fig. 6. Microstructure of the bismuth titanate films: (a) surface morphology of the films derived from acetylacetone route; (b) surface morphology of the films derived from acetic acid route; (c) cross-section showing well-developed grains ranging in size from 180 to 220 nm.

Films derived from an 'acetic acid' route showed a somewhat lower crystallinity. Both films were processed using multiple rapid thermal processing (MRTP), which consists in the processing of each layer. In this case each additional layer grows on an already crystallized bottom layer. As a result, the entire film composed from 4–5 layers appears more crystallized, giving rise to greater X-ray intensities. It is to be noted that the MRTP approach is efficient only when the grain growth occurs more rapidly than the nucleation. Films on the RuO_x substrate were well crystallized and no textured growth occurred, even though grains showed a slight preferential orientation in the $\{200\}$ direction (Fig. 5).

Deposited films were crack-free, uniform and adhered well on all tested substrates. It is to be noted that an extended heat-treatment in the temperature region 400–500°C often resulted in the micro-separation of a TiO_2 rich phase, causing low sample resistance. There was no remarkable difference in the surface morphology of films deposited on Pt or RuO_x substrates. The average grain size was estimated to be 170 nm (Fig. 6(a)). $\text{Bi}_4\text{Ti}_3\text{O}_{12}$ films derived from the 'acetic acid' route and processed under the same conditions showed less crystallinity, as also confirmed by X-ray diffraction. The average grain size from the picture was estimated to be around 100 nm (Fig. 6(b)). TEM cross-section of bismuth titanate film on an RuO_x electrode and processed at 700°C/30 s (MRTP) revealed well developed grains ranging in size from 170 to 220 nm (Fig. 6(c)). The columnar shape of the grains indicated that the nucleation started at the Pt/film interface, followed by rapid growth throughout the film thickness.

3.3 Electrical properties

3.3.1 Permittivity and ferroelectric properties

Figure 7 shows the dielectric properties of the films derived from the 'acetylacetone' route. The permittivity ϵ_r changed little for films processed at 700°C for 30 s on either Pt or RuO_x electrodes. Higher permittivities for the film MRTP processed at 700°C/180 s most likely arise from more crystallized sample. Permittivity values of the order of 200 are consistent with values reported by Joshi and Mansing,⁵ whereas other investigators report ϵ_r between 150 and 200.^{1,7} The dielectric loss factor was ≈ 0.01 at a frequency of 1 kHz.

The hysteresis loop of the bismuth titanate film on Pt is shown in Fig. 8. The values of saturation and remanent polarization of 22 and 11 $\mu\text{C}/\text{cm}^2$, respectively, indicated some *a*-axis component of polarization⁷ ($P_a = 50 \mu\text{C}/\text{cm}^2$, $P_c = 4 \mu\text{C}/\text{cm}^2$). A

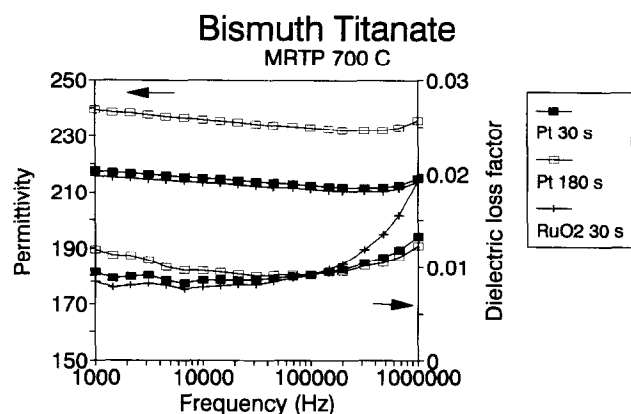


Fig. 7. Permittivity and dielectric loss factor of the bismuth titanate films processed at 700°C on Pt and ruthenium oxide electrodes. Longer holding times gave slightly higher permittivities.

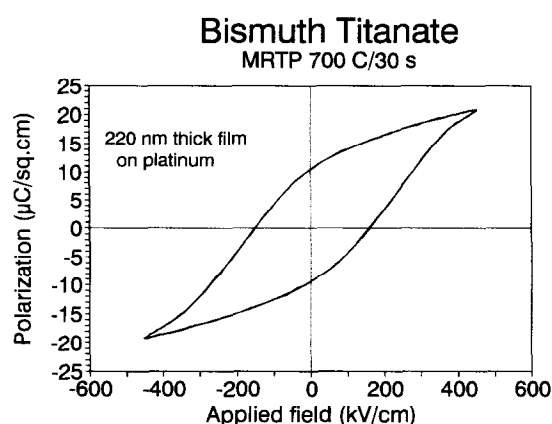


Fig. 8. Ferroelectric properties of the bismuth titanate films on Pt substrate. Slim loops observed up to an electric field of $E \approx 250$ kV/cm, remanent polarization $P_r = 11$ $\mu\text{C}/\text{cm}^2$, coercive field $E_c = 160$ kV/cm.

coercive force of the order of 160 kV/cm was measured.

3.3.2 Leakage current density

In ferroelectrics the conduction is electronic (*p*- or *n*-type) in nature arising from non-stoichiometry in the cation and/or oxygen concentration. In $\text{Bi}_4\text{Ti}_3\text{O}_{12}$, conduction can be *p*-type because of bismuth vacancies incurred during sintering or annealing. Defects and other impurities (Fe^{3+} , Cu^{2+} , etc.) can also contribute to the extrinsic conduction. The leakage current density (LCD) at room temperature of the $\text{Bi}_4\text{Ti}_3\text{O}_{12}$ films on Pt was of the order of 10 nA/cm² at an electric field of 60 kV/cm. As can be seen from a typical current–voltage (*I*–*V*) curve (Fig. 9) the slope of about 1 in the low-field region (up to 50 kV/cm) indicated an ohmic conduction mechanism. Above a critical field, the current increased abruptly owing to an emission mechanism (either Schottky or Poole–Frenkel). From the temperature dependence of conductivity, the activation energy of the conduction

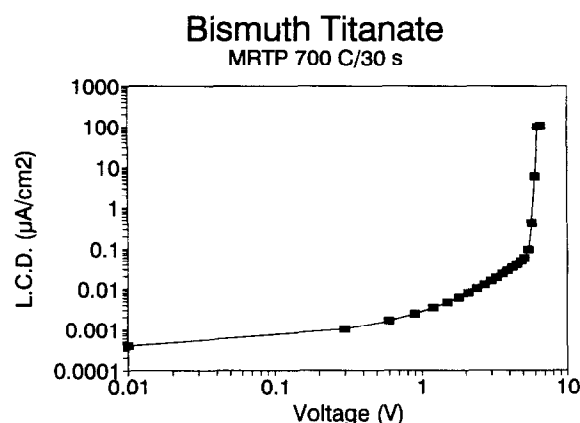


Fig. 9. Current–voltage characteristics of the bismuth titanate films show an ohmic type behaviour up to 180 kV/cm.

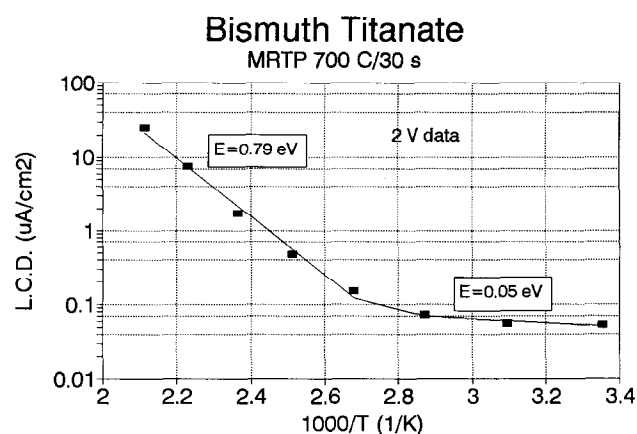


Fig. 10. Leakage current as a function of temperature of the bismuth titanate film, a lower activation energy of 0.8 eV in the high-temperature region suggests the presence of acceptor impurities.

process was derived. Figure 10 shows the steady-state leakage current as a function of $1/T$. The temperature dependence can be characterized by two regimes with very different activation energies. At low temperatures there was a weak temperature dependence with an activation energy of $E \approx 0.06$ eV. Above 90–100°C, the leakage current exhibited much stronger temperature dependence with an activation energy of $E \approx 0.8$ eV. A transition with an activation energy from 0.2 to 1.3 eV has been published for sol gel lead zirconate titanate films.¹¹ Bismuth vacancies and unintentionally introduced impurities are the main contributors to the generation of holes that are responsible for *p*-type conductivity. The near room-temperature activation energy of barely 0.06 eV could be consistent with the presence of a small number of shallow hole traps. Most of the holes are ‘frozen’ in deep hole traps as bismuth vacancies or transition metal impurities. With increasing temperature the hole concentration would increase because of thermal excitation. The concentration of untrapped holes

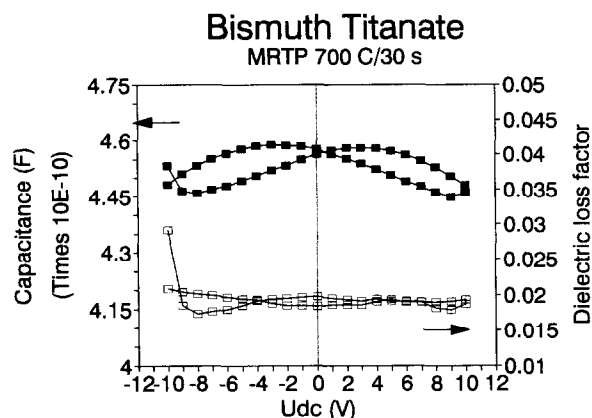


Fig. 11. Current-voltage characteristic of the bismuth titanate film. The capacitance remained almost constant over the voltage range -275 – $+275$ kV/cm.

could be decreased by using a proper donor dopant, providing that the concentration of the bismuth vacancies is lowered. The latter may be attained by using bismuth in excess and high purity materials.

3.3.3 Charge storage density

The capacitance-voltage (C - V) characteristic for 400 nm thick bismuth titanate film multiply processed at 700°C for 30 s is illustrated in Fig. 11. The presence of two peaks on either side of abscissa (dc bias) confirmed ferroelectric domain switching in the films even though a sample capacitance did not change appreciably with applied voltage. This fact may be of interest for dynamic random memory (DRAM) applications, where a flat dependence of capacitance on voltage is required. A practical DRAM capacitor requires¹² a leakage current density of $<3 \mu\text{A}/\text{cm}^2$ and a charge storage density of $>30 \text{ fC}/\mu\text{m}^2$. Charge storage densities Q_c were estimated from the C - V characteristics using the relationship $Q_c = \epsilon_0 \cdot \epsilon_r \cdot E$, where ϵ_0 is the permittivity of free space, ϵ_r is the relative permittivity, and E is the applied electric field. A charge density of $37 \text{ fC}/\mu\text{m}^2$ was obtained (Fig. 12) at an electric field of 200 kV/cm. The leakage current observed at this electric field was less than $1 \mu\text{A}/\text{cm}^2$.

4 CONCLUSION

1. Crystalline ferroelectric bismuth titanate films were reproducibly fabricated using a modified sol gel method. The process was simplified using stock titanium and bismuth solutions, which are easy to handle. A stable and clear bismuth titanate solution was prepared by a simple mixing of the stock

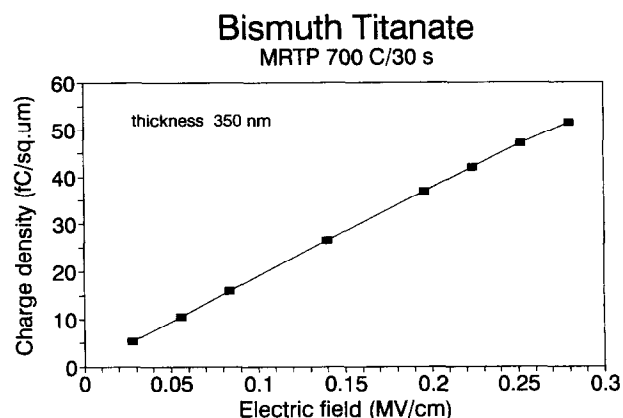


Fig. 12. Capacitance charge density as a function of applied voltage.

solutions and dilution with water. The preparation procedure of bismuth titanate solution need not be carried on under purge gas.

2. Multiple rapid thermal processing of each layer at 700°C for 30 s gave rise to fully crystallized films. Films with 3% of bismuth in excess did not show the presence of pyrochlore $\text{Bi}_2\text{O}_3 \cdot 2\text{TiO}_2$ phase. The average grain size of optimally processed films was of the order of 175 nm and grains grew through the thickness of the entire film.
3. The permittivity in a typical range of 230 and $\tan\delta$ 0.01 were measured. P - E hysteresis loops were observed with the ferroelectric properties of $P_s = 22 \mu\text{C}/\text{cm}^2$, $P_r = 11 \mu\text{C}/\text{cm}^2$ and the coercive force of $E_c = 160 \text{ kV}/\text{cm}$. The leakage current density was of the order of $10 \text{ nA}/\text{cm}^2$ at $60 \text{ kV}/\text{cm}$.

ACKNOWLEDGEMENTS

The work has been supported by the Natural Sciences and Engineering Research Council of Canada, the Ontario Centre for Materials Research, Northern Telecom Limited and Gennum Corporation. We would like to thank Mr P. Nolan for SEM studies, Dr L. Weaver for TEM studies and Ms J. Cooley for glancing angle data.

REFERENCES

1. BUHAY, H., SINHARROY, S., KASNER, W. H., FRANCOMBE, M. H., LAMPE, D. R. & STEPKE, E., *Appl. Phys. Lett.*, **58** (1991) 1470.
2. RAMESH, R., INAM, A., CHAN, W. K., WILKENS, B., MYERS, K., TEMSCHNIG, K., HART, D. L. & TARASCON, J. M., *Science*, **252** (1991) 944.

3. MAFFEI, N., KRUPANIDHI, S. B., *Appl. Phys. Lett.*, **60** (1992) 781.
4. SI, J. & DESU, S. B., *J. Appl. Phys.*, **73** (1993) 7911.
5. JOSHI, P. C. & MANSING, A., *Appl. Phys. Lett.*, **59** (1991) 2389.
6. TOHGE, N., FUKUDA, Y. & MINAMI, T., *Jpn J. Appl. Phys.*, **31** (1992) 4016.
7. TOYODA, M., HAMAJI, Y., TOMONO, K. & PAYNE, D. A., *Jpn J. Appl. Phys.*, **32** (1993) 4158.
8. SAYER, M. & SEDLAR, M., *Integrated Ferroelectrics*, **6-8** (1995).
9. SEDLAR, M. & SAYER, M., *J. Sol Gel Sci. Technol.* (submitted).
10. YI, G., PhD Thesis, Queen's University, Canada, 1993.
11. DIMOS, D., SCHWARTZ, R. W. & LOCKWOOD, S. J., *J. Am. Ceram. Soc.*, **77** (1994) 3000.
12. ROY, D., KRUPANIDHI, S. B., *Appl. Phys. Lett.*, **62** (1993) 1056.